ACS OMEGA

Open Access

http://pubs.acs.org/journal/acsodf

Article

Silapropofol: Carbon−Silicon Isosterism in a Key Anesthetic Scaffold

Sarah Koschabek, Florian Kleemiss, Noel Angel Espinosa-Jalapa, and Jonathan O. Bauer*

Cite This: *ACS Omega* 2026, 11, 3529−3534

Read Online

ACCESS | Metrics & More | Article Recommendations | Supporting Information

ABSTRACT: Propofol (2,6-di-*iso*-propylphenol) (**1**) is one of the most widely used intravenous anesthetics, yet its high lipophilicity, formulation challenges, and incompletely understood binding mode motivate the exploration of structural analogues. Here, we report the synthesis and comprehensive characterization of the first silicon analogues of propofol, monosilapropofol (**2**) and disilapropofol (**3**), in which one or both *iso*-propyl groups are replaced by dimethylsilyl substituents. Key steps involve optimized [1,3]-retro-Brook rearrangements, with *tert*-butyllithium-mediated Li/Br exchange enabling efficient access to both targets. Crystalline potassium phenolate **2-K** provided the first X-ray diffraction analysis of a silapropofol derivative, and complementary quantum chemical analysis based on orbital, topological, and localizability descriptors revealed pronounced polarization effects and bond umpolung in this pharmacologically relevant scaffold arising from carbon−silicon isosterism. Stability studies under physiological conditions uncovered a strong divergence between the two analogues: while **2** undergoes gradual hydrolysis to 2-*iso*-propylphenol and dimethylsilanol, **3** proved remarkably robust in neutral saline solution. These findings demonstrate that silicon substitution offers a powerful strategy to modulate both electronic properties and aqueous stability in propofol derivatives, highlighting carbon−silicon isosterism as a valuable concept for anesthetic drug design.

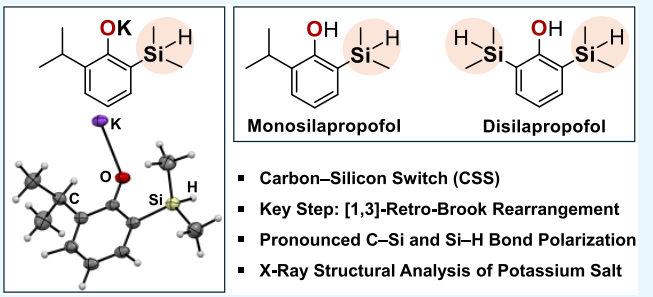

INTRODUCTION

Propofol (2,6-di-*iso*-propylphenol) (**1**, Figure 1) has been one of the most widely used intravenous anesthetics since its clinical introduction in the 1980s, and it is included in the World Health Organization's List of Essential Medicines.[1,2] It is routinely administered for the induction and maintenance of general anesthesia as well as for sedation in intensive care units, and it has gained particular importance during the COVID-19 pandemic in the context of long-term mechanical ventilation.[3,4] Propofol is valued for its rapid onset of action, smooth recovery profile, and relatively low incidence of postoperative nausea and vomiting. However, it lacks intrinsic analgesic activity and is associated with disadvantages such as severe injection pain and formulation challenges arising from its high lipophilicity and poor aqueous solubility.[5−7]

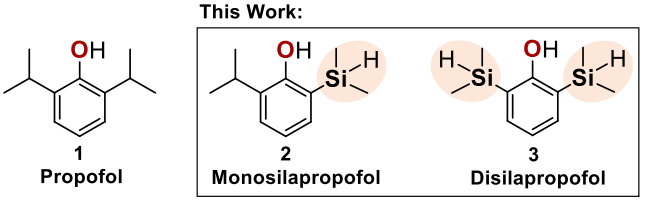

Figure 1. Concept of the carbon−silicon switch in propofol (**1**): replacement of one or both *iso*-propyl groups by dimethylsilyl groups affords the bioisosteric analogues monosilapropofol (**2**) and disilapropofol (**3**) synthesized in this study.

At the molecular level, propofol exerts its pharmacological effects primarily by allosteric modulation of γ-aminobutyric acid type A ($GABA_A$) receptors, the most important inhibitory ion channels in the central nervous system.[8,9] Structural studies have revealed that propofol binds within cavities of the transmembrane domain, where the *iso*-propyl substituents engage in van der Waals interactions and the phenolic hydroxy group forms hydrogen bonds to the receptor backbone.[10−13] Despite significant progress, the precise mechanisms of receptor modulation remain incompletely understood, underscoring the importance of systematic structure−activity investigations and the design of structurally modified analogues.

In this context, carbon−silicon isosterism has emerged as a powerful concept to probe and modulate molecular properties. The systematic replacement of a carbon atom by silicon—referred to as the carbon−silicon switch (CSS)—preserves the overall molecular framework due to the valence isoelectronic relationship of the two elements, while subtly increasing molecular volume as a result of the larger atomic radius of silicon.[14,15] More profound, however, are the electronic

Received: October 25, 2025
Revised: December 23, 2025
Accepted: December 25, 2025
Published: January 7, 2026

Scheme 1. General Synthetic Route to Monosilapropofol (2). Bromination of 2-*iso*-Propylphenol (4) Provides 2-Bromo-6-*iso*-Propylphenol (5). Subsequent Hydroxy Silylation Furnishes the Corresponding Silyl Ether (6), Which Undergoes an Intramolecular [1,3]-Retro-Brook Rearrangement to Deliver Monosilapropofol (2). Deprotonation with Potassium *tert*-Butoxide Affords the Crystalline Potassium Phenolate (2-K)

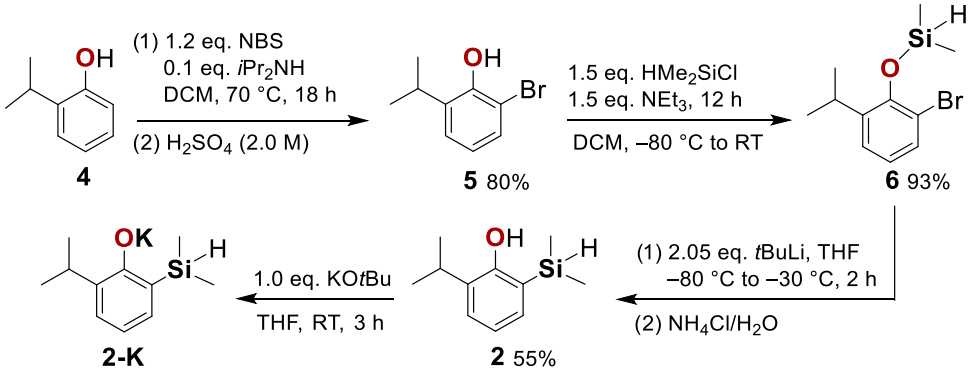

consequences: the lower electronegativity of silicon compared to carbon leads to altered bond polarities, including an inversion (umpolung) of the bond dipole in Si−H relative to C−H bonds.[16] Such differences in polarity and polarizability can significantly influence solvation behavior and molecular recognition in protein binding pockets, ultimately affecting pharmacological potency, selectivity, and pharmacokinetic properties.[14]

Although applications of sila analogues in medicinal chemistry are still comparatively limited, they have proven to be valuable tools for tuning biological properties and gaining insights into ligand−receptor interactions and metabolic stability. The potential of CSS has been demonstrated in several cases, including sila-ibuprofen,[17] sila-haloperidol,[18] sila-venlafaxine,[19] disila-bexarotene,[20] sila-loperamide,[21] and sila-1,4-dihydropyridine.[22] These examples illustrate how strategic incorporation of silicon into established drug scaffolds can enhance bioactivity or reveal novel pharmacological profiles.

Herein, we report the first synthesis of sila analogues of propofol (Figure 1). By replacing one or both *iso*-propyl substituents with dimethylsilyl groups, we have prepared monosilapropofol (**2**) and disilapropofol (**3**). Compound **2** was characterized by single-crystal X-ray diffraction analysis in the form of its potassium salt and by quantum chemical methods (QTAIM, NPA, NRT, ESP), enabling a detailed analysis of the structural and electronic consequences of C/Si substitution. Furthermore, the stability of the sila analogues **2** and **3** in aqueous media under physiological conditions was investigated, providing first insights into their potential as novel anesthetic agents.

RESULTS AND DISCUSSION

Synthesis of Monosilapropofol (2)

The synthesis of 2-(dimethylsilyl)-6-*iso*-propylphenol (**2**, monosilapropofol) was accomplished in a three-step sequence (Scheme 1).

The initial *ortho*-bromination of 2-*iso*-propylphenol (**4**) proceeded under Soxhlet conditions with *N*-bromosuccinimide (NBS) as the bromine source, following a modified literature protocol.[23] Control of the NBS stoichiometry proved to be essential for reproducibility: with one equivalent of NBS a conversion of 74% was achieved, whereas a slight excess (1.2 equiv) increased the conversion to 88%. After purification, the isolated material (80%) consisted of 94% 2-bromo-6-*iso*-propylphenol (**5**) and 6% unreacted starting material **4**.

In the second step, silylation of the hydroxy group was performed using chlorodimethylsilane (1.5 equiv) and triethylamine (1.5 equiv) in dichloromethane (DCM). The reaction afforded the expected silyl ether **6** in 94% purity alongside a minor byproduct (6%) of the corresponding silyl ether, which originated from residual **4** in the preceding step. Pure compound **6** was isolated in 93% yield after Kugelrohr distillation.

The key transformation was a [1,3]-retro-Brook rearrangement of compound **6**,[24−28] enabling migration of the dimethylsilyl moiety from oxygen to the *ortho*-carbon atom (Scheme 1). Initial experiments with one equivalent of *n*-butyllithium in tetrahydrofuran (THF) at −80 °C to −30 °C gave incomplete conversion, yielding 56% of **2** together with 44% of **5**, the latter arising from hydrolytic cleavage of unconverted starting material during workup (for details, see the Supporting Information, SI, Table S1). Direct warming from −80 °C to room temperature and prolonging the reaction time to 24 h further reduced the yield of **2** to 44%. Changing the solvent to diethyl ether applying temperatures from −80 °C to −30 °C gave no conversion. Employing a slight excess of *n*-butyllithium (1.1 equiv) in THF improved the conversion to give 60% of **2**. Significantly better results were obtained with *tert*-butyllithium as a base. When compound **6** was treated with 2.05 equiv of *tert*-butyllithium in THF at −80 °C, followed by gradual warming to −30 °C, the crude mixture contained 92% monosilapropofol (**2**) and only 8% of **5**. This result highlights the higher efficiency of Li/Br exchange under the stronger basicity of *tert*-butyllithium, favoring productive rearrangement.

Attempts to separate **2** from minor amounts of **5** by column chromatography were unsuccessful due to cleavage of the sensitive dimethylsilyl group, even when neutralized silica was employed. While Kugelrohr distillation did not afford significant additional purification, subsequent low-temperature precipitation (−80 °C) from *n*-hexane provided the target compound **2** as an amorphous solid in excellent purity, with an isolated yield of 55 % (Scheme 1). The reaction scale also influenced conversion efficiency: batches above 10 mmol exhibited reduced yields, presumably due to incomplete cooling and diffusion limitations, underscoring the importance of precise low-temperature control.

https://doi.org/10.1021/acsomega.5c11217
ACS Omega 2026, 11, 3529−3534

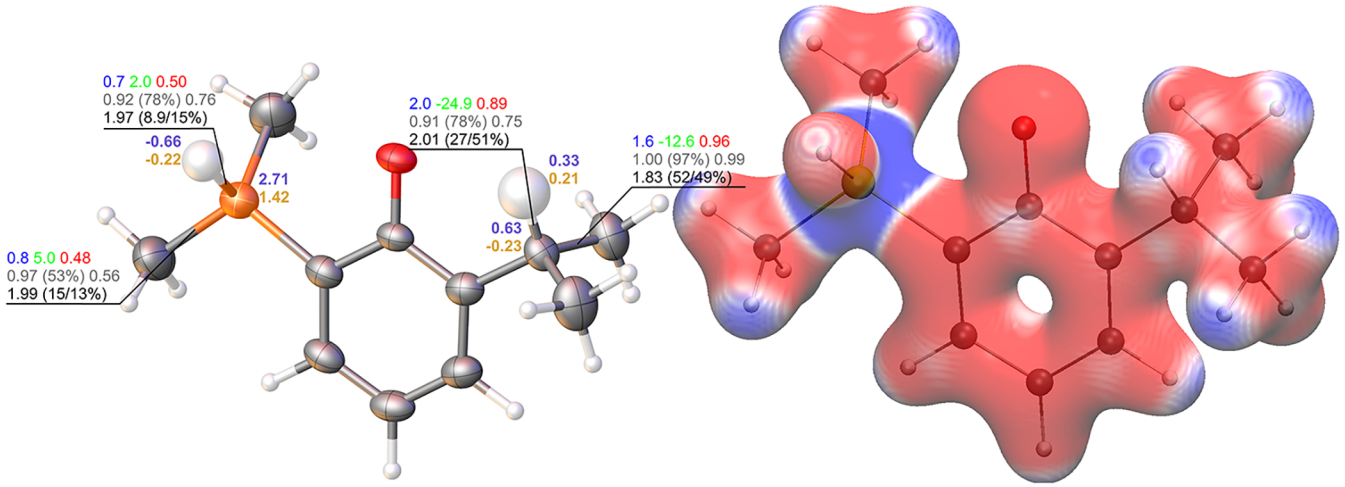

Figure 2. Left: Molecular structure of the potassium salt of the major disorder component of monosilapropofol (**2-K**) in the crystal (only anion shown). Anisotropic displacement parameters (ADPs) of non-hydrogen atoms are shown at the 80% probability level; hydrogen atoms are depicted at an arbitrary scale, with enlarged ADPs highlighting the discussed charge distribution. Bond descriptors are labeled according to the following color code: QTAIM charges (e, violet), NPA charges (e, yellow), electron density (ρ in eÅ^{-3}, blue) and Laplacian of the density ($\Delta\rho$ in eÅ^{-5}, green) at the bond critical point (BCP), delocalization index (red), NBO bond order with percentage weight of the covalent portion (in parentheses) and with NLMO/NPA bond order (gray), and population of the diatomic ELI-D basin with contribution from the higher-Z element to the bond given by volume/electron density (black). Right: Electrostatic potential (ESP) mapped onto the 0.001 au electron density isosurface, color-coded from −0.01 au (red) to +0.01 au (blue).

As monosilapropofol **2** is a liquid above −80 °C, it was unsuitable for single-crystal X-ray diffraction analysis. Although cocrystallization with isonicotinamide is known for propofol,[29] the same approach with **2** was unsuccessful, likely due to the reduced Lewis basicity of its phenolic hydroxy group caused by the carbon−silicon switch. To overcome this limitation and further probe its reactivity, alkali metal phenolates were prepared. Reaction with sodium *tert*-butoxide yielded only amorphous material, whereas treatment with potassium *tert*-butoxide furnished the crystalline potassium phenolate **2-K**, suitable for single-crystal X-ray diffraction analysis (Figure 2). Structural analysis based on the diffraction data revealed significant elongation of the C−Si bonds by ∼0.33 Å relative to the corresponding C−C bonds of the *iso*-propyl substituent, while bond angles remained essentially unchanged.

Bonding Analysis and Electrostatic Properties of 2-K

The carbon−silicon switch (CSS) offers a unique strategy to probe bioisosterism by altering electronic distribution while maintaining steric similarity.[30,31] Detailed quantum-chemical analyses of the molecular structure of **2-K** (ORCA 5.0, PBE/def2-TZVPPD)[32−37] provided insight into the electronic consequences of C/Si substitution (Figure 2).[38,39] Natural population analysis (NPA)[40] and quantum theory of atoms in molecules (QTAIM)[41] revealed the expected umpolung upon carbon−silicon switch: the hydrogen atom attached to silicon carried a net negative charge (−0.22 e NPA; −0.66 e QTAIM), in sharp contrast to the positively polarized hydrogen atom of the tertiary carbon atom of the *iso*-propyl group (+0.21 e NPA; + 0.33 e QTAIM). Similarly, the silicon atom exhibited strong positive polarization (1.42 e/2.71 e based on NPA/QTAIM), while the corresponding tertiary carbon atom displayed a weakly negative to slightly positive charge (−0.23 e/0.63 e based on NPA/QTAIM).

In addition to the pronounced charge redistribution, the bonding analysis reveals a fundamental difference between C−H and Si−H bonds. QTAIM descriptors (electron density and Laplacian at the bond critical point, and the delocalization index) indicate that the C−H bond in the *iso*-propyl group retains a highly covalent character, whereas the corresponding Si−H bond in the dimethylsilyl group is markedly more polarized, characterized by a positive Laplacian and a delocalization index below 0.5. This trend is corroborated by the Raub−Jansen index (RJI)[42] of the heavier element, which decreases from 51% for C−H to only 15% for Si−H, highlighting the electron density shift toward the hydrogen atom in the silyl function. A similar dichotomy is observed for the C−C versus Si−C bonds: in the *iso*-propyl fragment, high electron density, negative Laplacian, a delocalization index close to unity, and 97% covalency based on natural resonance theory (NRT)[43] analyses (49% according to RJI) collectively underscore an unpolarized covalent bonding situation. By contrast, the Si−C bond is substantially more polarized, displaying lower density, a positive Laplacian, a delocalization index of ∼0.5, and only 53% covalency according to NRT, which is further reflected in a significantly reduced RJI (<15%) (Figure 2).

The pronounced umpolung effect introduced by the carbon−silicon switch is also mirrored in the electrostatic potential (ESP) distribution, showing a positive region around the hydrogen atom of the tertiary carbon atom but a negative region around the silicon-bound hydrogen atom. Conversely, the ESP around the tertiary carbon atom is shifted to negative values, while the silicon atom itself adopts a positive potential. This inversion of local electrostatics underscores the unique capacity of carbon−silicon isosterism to tune bond polarity and electronic surface properties without altering the overall steric framework. Such changes are expected to influence interactions with receptor sites substantially.

Stability of Monosilapropofol (2) in Aqueous Solution

The hydrolytic stability of **2** was investigated under simulated physiological conditions (for details, see the SI, Section 2.5). In 0.9% NaCl/D_2O at room temperature, ^{1}H NMR spectra showed a gradual decomposition from 98% purity initially to 78% after 2 weeks and near-complete hydrolysis after 6 weeks.

https://doi.org/10.1021/acsomega.5c11217
ACS Omega 2026, 11, 3529−3534

Scheme 2. General Synthetic Route to Disilapropofol (3). Successive Hydroxy Silylation and [1,3]-Retro-Brook Rearrangement Enable Exchange of Both Bromine Substituents in 2,6-Dibromophenol (7), Ultimately Affording Disilapropofol (3)

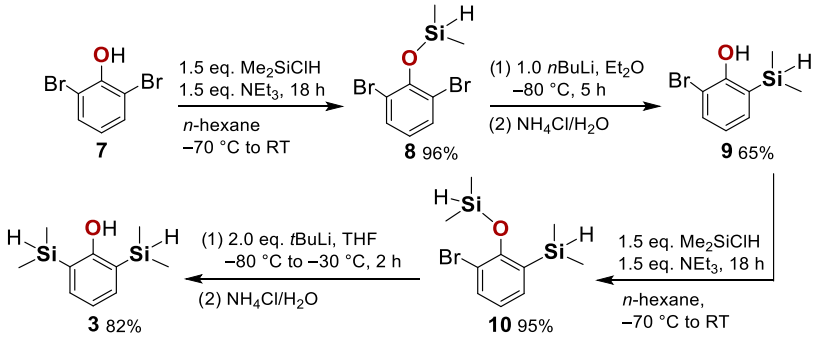

Under mildly basic conditions (10 mM $NaHCO_3/D_2O$, pH ≈ 8), decomposition was significantly faster: After 4 days, only 60% of **2** remained, accompanied by progressively broadened NMR signals, indicative of ongoing decomposition. The NMR spectra do not allow for an unambiguous assignment of the decomposition products. However, the still observable Si−H signal indicates that dimethylsilanol is likely formed as one of the hydrolysis products, together with 2-*iso*-propylphenol and other unidentified side products.

Synthesis of Disilapropofol (3)

Encouraged by the successful synthesis of **2**, we pursued the preparation of 2,6-bis(dimethylsilyl)phenol (**3**, disilapropofol) (Scheme 2). Irrespective of the specific pharmacological relevance of disilapropofol, 2,6-bis(trimethylsilyl)phenyl triflates have recently attracted considerable attention as precursors to silylbenzynes, which display unique and remarkable reactivity.[44]

The sequence commenced with the silylation of 2,6-dibromophenol (**7**), furnishing the corresponding dimethylsilyl ether **8** in 96% isolated yield. Subsequent [1,3]-retro-Brook rearrangement of **8** provided 2-bromo-6-(dimethylsilyl)phenol (**9**), with the conversion strongly dependent on base and solvent (for details, see the SI, Table S2). Treatment with *tert*-butyllithium promoted double Li/Br exchange, leading not only to the formation of compound **9** but also to 2-(dimethylsilyl)phenol as a byproduct, consistent with over-lithiation. Analogous to the behavior observed with *tert*-butyllithium, diethyl ether afforded higher conversion to **9** (66%) than THF (25%) at low temperature (−80 °C to −30 °C), which can be rationalized by the weaker stabilization of multiply charged intermediates in diethyl ether, thereby suppressing excessive Li/Br exchange and byproduct formation. By contrast, reactions with *n*-butyllithium resulted in only a single Li/Br exchange, giving **9** alongside unreacted **7** after aqueous workup. The best conversion to **9** (82%) was achieved in diethyl ether at low temperature (−80 °C), whereas THF under prolonged room temperature conditions led to considerably lower conversion (36%). Crude mixtures were subjected to Kugelrohr distillation; however, complete separation was not feasible due to the nearly identical molecular weights and boiling points of the components. Under the optimized conditions, a mixture of **9** (86%) and **7** (14%) was obtained as a colorless liquid after distillation. Subsequent recrystallization from *n*-hexane at −80 °C afforded colorless needles of **7**[45] and, in this way, pure compound **9** in 65% isolated yield (Scheme 2).

Silylation of **9** under standard conditions afforded the pure silyl ether **10** in 95% isolated yield. The final step toward disilapropofol (**3**) involved a [1,3]-retro-Brook rearrangement of **10**. Under the conditions previously optimized for the monosilyl analogue **9** (*n*-butyllithium in diethyl ether, −80 °C), conversion to **3** proved minimal (4%). In contrast, treatment of **10** with *tert*-butyllithium (2.0 equiv) in THF at −80 °C, followed by warming to −30 °C, furnished a mixture of **3** (97%), **9** (1%), and 2-(dimethylsilyl)phenol (2%), from which pure compound **3** was isolated in 82% yield after Kugelrohr distillation (Scheme 2).

Stability of Disilapropofol (3) in Aqueous Solution

The aqueous stability of **3** was examined in direct analogy to **2** (for details, see the SI, Section 2.10). Remarkably, **3** displayed superior stability under neutral conditions: no significant decomposition was observed in 0.9% $NaCl/D_2O$ at room temperature over 6 weeks. Under basic conditions (10 mM $NaHCO_3/D_2O$), however, decomposition occurred more rapidly, with 80% **3** remaining after 4 days and only 30% after 2 weeks. The NMR spectra do not allow for an unambiguous assignment of the decomposition products.

CONCLUSIONS

Monosilapropofol (**2**) and disilapropofol (**3**) were synthesized via optimized [1,3]-retro-Brook rearrangements in good yields and excellent purities. Comprehensive structural characterization, including single-crystal X-ray diffraction analysis of **2-K**, together with advanced quantum chemical analyses, revealed that carbon−silicon substitution profoundly alters bond polarity and the electrostatic potential while preserving steric similarity. We anticipate that **2** and **3** exhibit enhanced solubility in aqueous media compared to propofol, likely resulting from the increased polarity introduced by the carbon−silicon substitution, while showing slightly reduced lipophilicity. Aqueous stability studies underscored the impact of silicon substitution: monosilapropofol (**2**) undergoes gradual hydrolysis under physiological conditions, whereas disilapropofol (**3**) remains stable in neutral saline solution for weeks. Collectively, these findings highlight carbon−silicon isosterism as a powerful design principle in anesthetic chemistry and provide a foundation for the future development of silaprodrugs and silicon-based bioisosteres. Ongoing studies will address the pharmacological consequences of the carbon−silicon switch in propofol analogues, including receptor binding investigations. Importantly, the silicon analogues are not intended primarily to produce a more potent drug than

https://doi.org/10.1021/acsomega.5c11217
ACS Omega 2026, 11, 3529−3534

propofol, but rather to serve as versatile tools for probing its mechanism of action, investigating ligand−receptor interactions, and studying structure−activity relationships.

■ ASSOCIATED CONTENT

Supporting Information

The Supporting Information is available free of charge at https://pubs.acs.org/doi/10.1021/acsomega.5c11217.

Synthetic procedures, NMR spectra, quantum chemical details, X-ray crystallographic data (PDF)

Accession Codes

CCDC 2492470 contains the supplementary crystallographic data for this paper. These data can be obtained free of charge via www.ccdc.cam.ac.uk/data_request/cif, or by emailing data_request@ccdc.cam.ac.uk, or by contacting The Cambridge Crystallographic Data Centre, 12 Union Road, Cambridge CB2 1EZ, U.K.; fax: + 44 1223 336033.

■ AUTHOR INFORMATION

Corresponding Author

Jonathan O. Bauer − *Faculty of Chemistry and Pharmacy, Institute of Inorganic Chemistry, University of Regensburg, D-93053 Regensburg, Germany;* orcid.org/0000-0002-9575-7430; Email: jonathan.bauer@ur.de

Authors

Sarah Koschabek − *Faculty of Chemistry and Pharmacy, Institute of Inorganic Chemistry, University of Regensburg, D-93053 Regensburg, Germany*

Florian Kleemiss − *Department of Chemistry, Institute of Inorganic Chemistry, RWTH Aachen University, D-52074 Aachen, Germany;* orcid.org/0000-0002-3631-1535

Noel Angel Espinosa-Jalapa − *Faculty of Chemistry and Pharmacy, Institute of Inorganic Chemistry, University of Regensburg, D-93053 Regensburg, Germany*

Complete contact information is available at: https://pubs.acs.org/10.1021/acsomega.5c11217

Notes

The authors declare no competing financial interest.

■ ACKNOWLEDGMENTS

J.O.B. thanks the Elite Network of Bavaria (ENB) and the Bavarian State Ministry of Science and the Arts (StMWK) for financial support (Project N-LW-NW-2016-366).

■ REFERENCES

(1) Sahinovic, M. M.; Struys, M. M. R. F.; Absalom, A. R. Clinical Pharmacokinetics and Pharmacodynamics of Propofol. *Clin. Pharmacokinet.* **2018**, *57*, 1539−1558.

(2) World Health Organization. *World Health Organization Model List of Essential Medicines: 21st List*; WHO: Technical Document, Geneva, Switzerland, 2019; Vol. *2019*.

(3) Lewis, S. R.; Schofield-Robinson, O. J.; Alderson, P.; Smith, A. F. Propofol for the promotion of sleep in adults in the intensive care unit. *Cochrane Database Syst. Rev.* **2018**, No. CD012454.

(4) Hirota, K.; Lambert, D. G. Propofol and SARS-CoV-2 infection. *Br. J. Anaesth.* **2020**, *125*, e475−e476.

(5) Baker, M. T.; Naguib, M. Propofol: The Challenges of Formulation. *Anesthesiology* **2005**, *103*, 860−876.

(6) Momot, K. I.; Kuchel, P. W.; Chapman, B. E.; Deo, P.; Whittaker, D. NMR Study of the Association of Propofol with Nonionic Surfactants. *Langmuir* **2003**, *19*, 2088−2095.

(7) Hart, B. Diprivan': a change of formulation. *Eur. J. Anaesthesiol.* **2000**, *17*, 71−73.

(8) Jayakar, S. S.; Dailey, W. P.; Eckenhoff, R. G.; Cohen, J. B. Identification of Propofol Binding Sites in a Nicotinic Acetylcholine Receptor with a Photoreactive Propofol Analog. *J. Biol. Chem.* **2013**, *288*, 6178−6189.

(9) Alexander, S. P. H.; Benson, H. E.; Faccenda, E.; Pawson, A. J.; Sharman, J. L.; Catterall, W. A.; Spedding, M.; Peters, J. A.; Harmar, A. J. CGTP Collaborators. The Concise Guide to Pharmacology 2013/14: Ion Channels. *Br. J. Pharmacol.* **2013**, *170*, 1607−1651.

(10) Yip, G. M. S.; Chen, Z.-W.; Edge, C. J.; Smith, E. H.; Dickinson, R.; Hohenester, E.; Townsend, R. R.; Fuchs, K.; Sieghart, W.; Evers, A. S.; Franks, N. P. A propofol binding site on mammalian $GABA_A$ receptors identified by photolabeling. *Nat. Chem. Biol.* **2013**, *9*, 715−720.

(11) Bocquet, N.; Prado de Carvalho, L.; Cartaud, J.; Neyton, J.; Le Poupon, C.; Taly, A.; Grutter, T.; Changeux, J.-P.; Corringer, P.-J. A prokaryotic proton-gated ion channel from the nicotinic acetylcholine receptor family. *Nature* **2007**, *445*, 116−119.

(12) Nury, H.; Van Renterghem, C.; Weng, Y.; Tran, A.; Baaden, M.; Dufresne, V.; Changeux, J.-P.; Sonner, J. M.; Delarue, M.; Corringer, P.-J. X-ray structures of general anaesthetics bound to a pentameric ligand-gated ion channel. *Nature* **2011**, *469*, 428−431.

(13) Kim, J. J.; Gharpure, A.; Teng, J.; Zhuang, Y.; Howard, R. J.; Zhu, S.; Noviello, C. M.; Walsh, R. M., Jr; Lindahl, E.; Hibbs, R. E. Shared structural mechanisms of general anaesthetics and benzodiazepines. *Nature* **2020**, *585*, 303−308.

(14) Schwarz, J. *Atypical Elements in Drug Design*; Springer International Publishing: Cham, Switzerland, 2016.

(15) Bains, W.; Tacke, R. Silicon chemistry as a novel source of chemical diversity in drug design. *Curr. Opin. Drug Discovery Devel.* **2003**, *6*, 526−543.

(16) Seebach, D. Methods of Reactivity Umpolung. *Angew. Chem., Int. Ed., Engl.* **1979**, *18*, 239−258.

(17) Kleemiss, F.; Justies, A.; Duvinage, D.; Watermann, P.; Ehrke, E.; Sugimoto, K.; Fugel, M.; Malaspina, L. A.; Dittmer, A.; Kleemiss, T.; Puylaert, P.; King, N. R.; Staubitz, A.; Tzschentke, T. M.; Dringen, R.; Grabowsky, S.; Beckmann, J. Sila-Ibuprofen. *J. Med. Chem.* **2020**, *63*, 12614−12622.

(18) Tacke, R.; Heinrich, T.; Bertermann, R.; Burschka, C.; Hamacher, A.; Kassack, M. U. Sila-haloperidol: A Silicon Analogue of the Dopamine (D_2) Receptor Antagonist Haloperidol. *Organometallics* **2004**, *23*, 4468−4477.

(19) Daiss, J. O.; Burschka, C.; Mills, J. S.; Montana, J. G.; Showell, G. A.; Warneck, J. B. H.; Tacke, R. Sila-venlafaxine, a Sila-Analogue of the Serotonin/Noradrenaline Reuptake Inhibitor Venlafaxine: Synthesis, Crystal Structure Analysis, and Pharmacological Characterization. *Organometallics* **2006**, *25*, 1188−1198.

(20) Daiss, J. O.; Burschka, C.; Mills, J. S.; Montana, J. G.; Showell, G. A.; Fleming, I.; Gaudon, C.; Ivanova, D.; Gronemeyer, H.; Tacke, R. Synthesis, Crystal Structure Analysis, and Pharmacological Characterization of Disila-bexarotene, a Disila-Analogue of the RXR-Selective Retinoid Agonist Bexarotene. *Organometallics* **2005**, *24*, 3192−3202.

(21) Geyer, M.; Wellner, E.; Jurva, U.; Saloman, S.; Armstrong, D.; Tacke, R. Can Silicon Make an Excellent Drug Even Better? An in vitro and in vivo Head-to-Head Comparison between Loperamide and Its Silicon Analogue Sila-Loperamide. *ChemMedChem* **2015**, *10*, 911−920.

(22) Barth, E. R.; Längle, D.; Wesseler, F.; Golz, C.; Krupp, A.; Schade, D.; Strohmann, C. Higher Carbon Analogues of 1,4-Dihydropyridines as Potent TGFβ/Smad Inhibitors. *Eur. J. Inorg. Chem.* **2020**, 176−181.

(23) Velder, J.; Robert, T.; Weidner, I.; Neudörfl, J.-M.; Lex, J.; Schmalz, H.-G. Modular Synthesis of Chiral Phosphine-Phosphite-Ligands from Phenolic Precursors: A New Approach to Bidentate

Chelate Ligands Exploiting a P−O to P−C Migration Rearrangement. *Adv. Synth. Catal.* **2008**, *350*, 1309−1315.
(24) Brook, A. G. Some Molecular Rearrangements of Organosilicon Compounds. *Acc. Chem. Res.* **1974**, *7*, 77−84.
(25) Brook, A. G. Isomerism of Some α-Hydroxysilanes to Silyl Ethers. *J. Am. Chem. Soc.* **1958**, *80*, 1886−1889.
(26) Linderman, R. J.; Ghannam, A. Synthetic Utility and Mechanistic Studies of the Aliphatic Reverse Brook Rearrangement. *J. Am. Chem. Soc.* **1990**, *112*, 2392−2398.
(27) Nakazaki, A.; Nakai, T.; Tomooka, K. Asymmetric Retro-[1,4] Brook Rearrangement and Its Stereochemical Course at Silicon. *Angew. Chem., Int. Ed.* **2006**, *45*, 2235−2238.
(28) Xu, Y.; Xu, W.; Chen, X.; Luo, X.; Lu, H.; Zhang, M.; Yang, X.; Deng, G.; Liang, Y.; Yang, Y. $Me_3SiSiMe_2(O^nBu)$: a disilane reagent for the synthesis of diverse silacycles *via* Brook- and retro-Brook-type rearrangement. *Chem. Sci.* **2021**, *12*, 11756−11761.
(29) McKellar, S. C.; Kennedy, A. R.; McCloy, N. C.; McBride, E.; Florence, A. J. Formulation of Liquid Propofol as a Cocrystalline Solid. *Cryst. Growth Des.* **2014**, *14*, 2422−2430.
(30) Arabi, A. A.; Matta, C. F. Electrostatic Potentials and Average Electron Densities of Bioisosteres in Methylsquarate and Acetic Acid. *Future Med. Chem.* **2016**, *8*, 361−371.
(31) Meanwell, N. A. Synopsis of Some Recent Tactical Application of Bioisosteres in Drug Design. *J. Med. Chem.* **2011**, *54*, 2529−2591.
(32) Perdew, J. P.; Burke, K.; Ernzerhof, M. Generalized Gradient Approximation Made Simple. *Phys. Rev. Lett.* **1996**, *77*, 3865−3868.
(33) Weigend, F.; Ahlrichs, R. Balanced Basis Sets of Split Valence, Triple Zeta Valence and Quadruple Zeta Valence Quality for H to Rn: Design and Assessment of Accuracy. *Phys. Chem. Chem. Phys.* **2005**, *7*, 3297−3305.
(34) Neese, F. The ORCA Program System. *WIREs Comput. Mol. Sci.* **2012**, *2*, 73−78.
(35) Neese, F.; Wennmohs, F.; Becker, U.; Riplinger, C. The ORCA Quantum Chemistry Program Package. *J. Chem. Phys.* **2020**, *152* (22), No. 224108.
(36) Kleemiss, F.; Dolomanov, O. V.; Bodensteiner, M.; Peyerimhoff, N.; Midgley, L.; Bourhis, L. J.; Genoni, A.; Malaspina, L. A.; Jayatilaka, D.; Spencer, J. L.; White, F.; Grundkötter-Stock, B.; Steinhauer, S.; Lentz, D.; Puschmann, H.; Grabowsky, S. Accurate crystal structures and chemical properties from NoSpherA2. *Chem. Sci.* **2021**, *12*, 1675−1692.
(37) Neese, F. Software Update: Software update: The ORCA program system—Version 5.0. *WIREs Comput. Mol. Sci.* **2022**, *12*, No. e1606.
(38) Woińska, M.; Grabowsky, S.; Dominiak, P. M.; Woźniak, K.; Jayatilaka, D. Hydrogen atoms can be located accurately and precisely by x-ray crystallography. *Sci. Adv.* **2016**, *2*, No. e1600192.
(39) Sanjuan-Szklarz, W. F.; Woińska, M.; Domagała, S.; Dominiak, P. M.; Grabowsky, S.; Jayatilaka, D.; Gutmann, M.; Woźniak, K. On the accuracy and precision of X-ray and Neutron diffraction results as a function of resolution and the electron density model. *IUCrJ.* **2020**, *7*, 920−933.
(40) Weinhold, F.; Landis, C. R. *Valency and Bonding: A Natural Bond Orbital Donor-Acceptor Perspective*; Cambridge University Press: Cambridge, U.K., 2005.
(41) Bader, R. F. W. *Atoms in Molecules: A Quantum Theory*; Clarendon Press: Oxford, U.K., 1994.
(42) Raub, S.; Jansen, G. A quantitative measure of bond polarity from the electron localization function and the theory of atoms in molecules. *Theor. Chem. Acc.* **2001**, *106*, 223−232.
(43) Glendening, E. D.; Landis, C. R.; Weinhold, F. Resonance Theory Reboot. *J. Am. Chem. Soc.* **2019**, *141*, 4156−4166.
(44) Ikawa, T.; Nishiyama, T.; Shigeta, T.; Mohri, S.; Morita, S.; Takayanagi, S.; Terauchi, Y.; Morikawa, Y.; Takagi, A.; Ishikawa, Y.; Fujii, S.; Kita, Y.; Akai, S. *ortho*-Selective Nucleophilic Addition of Primary Amines to Silylbenzynes: Synthesis of 2-Silylanilines. *Angew. Chem., Int. Ed.* **2011**, *50*, 5674−5677.
(45) Bauer, J. O.; Koschabek, S.; Falk, A. Interplay of Hydrogen and Halogen Bonding in the Crystal Structures of 2,6-Dihalogenated Phenols. *ChemistrySelect* **2021**, *6*, 8736−8740.

https://doi.org/10.1021/acsomega.5c11217
ACS Omega 2026, 11, 3529−3534